

ON THE MODELING OF COUPLING FAILURES IN LAMINATED COMPOSITE

Minh-Quan Le¹, Pierre Ladevèze¹, David Néron¹, Cuong Ha-Minh¹

¹LMT, ENS Paris-Saclay, CNRS, Université Paris-Saclay, 61 Avenue du Président Wilson, 94235
Cachan cedex, France

Email: {ladeveze,le,neron,haminh,}@lmt.ens-cachan.fr

Keywords: laminates, matrix cracking, delamination, coupling, damage mesomodel

Abstract

In order to establish a reliable virtual testing strategy for composite design, the damage mesomodel for laminated composites has been developed at LMT-Cachan since the 1980s. The new version of the mesomodel has been recently proposed to make a physically sound prediction of composite structures involving extensive splitting. It distinguishes diffuse transverse microcracking modeled by a homogenized procedure from splits observed as isolated mesocracks where a discontinuous approach is more appropriate. A split detection criterion is proposed for the split locations and cohesive interfaces are introduced for representing split process in interaction with delamination interfaces. This version has been developed and validated through comparisons with numerous available tests. The computational results show a very good correlation with the experiments.

1. Introduction

The modern structural design has witnessed a wide application of composite materials due to their outstanding properties as well as design flexibility, especially in the aeronautic and spacial industries. However, the manufacturing of such structures may require numerous experimental tests from component to full scale which are expensive in economics. Therefore, the virtual testing, whose goal is to drastically reduce the huge number of industrial tests involved in current characterization procedures, constitutes one of today's main industrial challenges. An answer to these challenges is what we call "damage mesomodel for laminated composite", developed at LMT-Cachan since the 1980s. The mesomodel is able to describe different micromechanical phenomena of composite degradation at the mesolevel via a homogenized representation such as fiber/matrix debonding, transverse microcracking, delamination and fiber breakage. The interaction between delamination and transverse microcracking has been also taken in account to allow a physically sound description.

In some particular situations involving extensive splits, predictions using the mesomodel result in too conservative strength probably leading to an oversized structure design. The reason has been found that the calculated splits can be too thick compared to experimental observations. In fact, split and transverse microcracking are both intraply matrix failure at the ply scale. However, while transverse microcracking is seen as distributed phenomenon in which a homogenization is suitable for modeling, split is referred to as an extremely thin and relatively isolated matrix crack spreading in parallel with fiber direction where a homogenized representation is no longer appropriate. Moreover, the presence of extensive splits is quite important since they are able to aggravate damage process and are part of global structure failure. Therefore, the split modeling is absolutely indispensable where discontinuous approaches such as cohesive interfaces or XFEM-based tools are often preferred. The mesomodel can predict correctly split onset but fails to represent split propagation, particularly extensive split. A new mesomodel-based approach has been thus completed to deal with the split modeling in order to improve the predictive capability of the mesomodel in some composite structures involving extensive splitting. The main idea

is to remark that until split initiation, the mesomodel and its numerical implementation do not involve any difficulty since there is no the discrete phenomenon. Once the split onset is first detected in a ply, a discontinuous approach is then used by inserting a cohesive interface orthogonal to the ply plane with the height equal to the ply thickness and parallel to the fibre direction. Apart from the split detection, the transverse microcracking are homogenously represented over the different plies via a density variable. One should be noted that it is preferred to homogenize transverse microcracking since a discrete representation of all straight transverse microcracks can lead to a huge computational capability, particularly for large industrial structures. Furthermore, the exact location of individual transverse microcracks is not important to the structure failure. However, their presence can trigger delamination due to the stress concentration in the interface that was taken in account by the mesomodel. A shear-based criterion for splitting detection has been also proposed for avoiding to introduce a priori interface elements in all plies that is not objective in the sense of the prediction. Nevertheless, it should be noticed that the use of cohesive elements requires predefined crack locations that can be detected by the split detection criterion and a mesh that is aligned with the crack path. Even though the use of XFEM or its variants could be efficient, the choice of interface elements were decided in this study because it is a sole option in the SAMCEF commercial finite element code in which the mesomodel was natively incorporated.

The aim of this paper is to demonstrate the coupling between intraply matrix cracks (splits and transverse microcracking) and interface delamination leading to different failure modes of laminated composite structures thanks to the new approach. It has been found in the literature that there are two principal failure modes : fiber and matrix dominated failures. Particularly, the later issues from a quite complex coupling such that structures manifest several major local instabilities before the fatal fracture. Simulations have been realized in connection with the experiments carried out by Kortschot et al. on double-edge-notched laminates for fiber dominated failure and by Hallett et al. on holed composite structures for matrix dominated one. The mesomodel is briefly reviewed in Section 2 with the split detection criterion. Finally, the computational results showing a very good correlation with the experiments are presented in Section 3.

2. Mesomodel of damage mechanism in laminated composites

This section presents briefly the mesomodel. More details can be found in [1].

2.1. A brief review of the mesomodel

Two main assumptions must be noticed: firstly, a laminate could be described as a stacking sequence of homogeneous plies and of interlaminar interfaces; secondly, an uniform damage state is prescribed throughout the thickness of elementary ply but it can vary from ply-to-ply. The mesomodel describes different micromechanical phenomena of degradation via a thermodynamically consistent damage homogenization. These phenomena can be classified into the following elementary damage mechanisms consisting on the their characterized scales. For the ply:

- Diffuse damage, characterized on the fiber's scale, is related to fibre/matrix debonding or deterioration of matrix between fibers;
 - Diffuse transverse microcracking, characterized at the ply's scale, represents straight through-ply-thickness cracks showing a quasi-uniform distribution;
 - Fiber breaking, generally leading to the final fracture of structures, is a catastrophic mechanism;
- and for the interface:
- Diffuse interface damage related to small-scale cracking within the matrix- rich interface layer;
 - Localized delamination caused by stress concentrations at the tips of the transverse matrix cracks.

Constitutive behavior of the ply. The potential energy density of the damaged ply E_D can be defined as:

$$\begin{aligned}
 2E_D = & \frac{1}{(1-d_f)E_1^o} \left[\langle \sigma_{11} \rangle^2 + \Phi(\langle -\sigma_{11} \rangle) - 2\nu_{12}^o \sigma_{11} \sigma_{22} - 2\nu_{13}^o \sigma_{11} \sigma_{33} \right] \\
 & + \left[\frac{\langle -\sigma_{22} \rangle^2}{E_2^o} + \frac{\langle -\sigma_{33} \rangle^2}{E_3^o} - \left(\frac{\nu_{23}^o}{E_2^o} + \frac{\nu_{32}^o}{E_3^o} \right) \sigma_{22} \sigma_{33} \right] + \left[\frac{\langle \sigma_{22} \rangle^2}{E_2^o (1-d')(1-\bar{d}_{22})} + \frac{\langle \sigma_{33} \rangle^2}{E_3^o (1-d')} \right] \\
 & + \left[\frac{\sigma_{12}^2}{G_{12}^o (1-d)(1-\bar{d}_{12})} + \frac{\sigma_{23}^2}{G_{23}^o (1-d_{23})(1-\bar{d}_{23})} + \frac{\sigma_{13}^2}{G_{13}^o (1-d)} \right] \quad (1)
 \end{aligned}$$

- d_f is the damage variable describing fibre breaking;
- $d, d', d_{23} = f(d')$ are the damage variables representing the diffuse damage;
- $\bar{d}_{22}, \bar{d}_{12}, \bar{d}_{23}$ are the damage variables due to transverse matrix cracking;
- Φ is the function which accounts for the nonlinear elastic response in compression;
- E_i^o is initial elastic modulus of the ply in the i direction
- G_{ij}^o is initial shear modulus of the ply in the $i-j$ plane ($i, j = 1, 2, 3$ and $i \neq j$);
- σ_{ij}^o is the axial stress in the i direction ($i = j$) or in the $i-j$ plane ($i \neq j$)
- $\langle \blacksquare \rangle$ designates the positive part which accounts for the crack opening or closure.

By deriving the potential energy density with respect to each damage variable, one can obtain its associated thermodynamic forces which are analogous to energy release rates:

$$Y_D = \frac{\partial}{\partial D} \langle \langle E_D \rangle \rangle_{|\sigma} \quad (2)$$

where $\langle \langle \blacksquare \rangle \rangle$ designates the mean value through the ply thickness, D stands for $d_f, d, d', d_{23}, \bar{d}_{22}, \bar{d}_{12}, \bar{d}_{23}$. Each elementary damage mechanism is modeled separately. However, within each of them (fiber breaking, diffuse damage, transverse microcracking), thermodynamic forces can interact with each other under the form of the effective driving force \bar{Y} to govern the damage evolution:

$$Y_D = f(\bar{Y}) \quad (3)$$

Constitutive behavior of the interface. The interface is modeled by the 2D entity in which the two in-plane axes are defined by the bisectors of the angles between fibre directions of the adjacent plies and the third is normal to the interface. The potential energy density per unit area e_D is then defined as:

$$2e_D = h_I \left[\frac{\langle -\sigma_{33} \rangle^2}{E^o} + \frac{\langle \sigma_{33} \rangle^2}{E^o (1-d_{33})} + \frac{\sigma_{13}^2}{G^o (1-d_{13})} + \frac{\sigma_{23}^2}{G^o (1-d_{23})} + \frac{\omega}{G^o} \sigma_{13} \sigma_{23} \right] \quad (4)$$

where h_I is the interface thickness, E^o and G^o are respectively the initial elastic and shear moduli of the interface, d_{33}, d_{13}, d_{23} are the damage variables associated with the Mode I, II and III respectively, ω is the coupling term. The damage evolution is governed by the effective thermodynamic force \bar{Y}_I accounting for a mixed-mode delamination. The evolution law is modeled by the function ℓ which is able to describe the interfacial stiffness degradation affected by diffuse interface damage. Furthermore, the effect of transverse microcracking in the adjacent plies can be modeled as seen in Eq. 5. According to [2], delamination process typically occurs at the saturation microcrack density ρ_s . When the density is at the saturation, the interface is completely damaged as seen in Eq.6.

- for $\rho < \rho_s$

$$d_{33} = \ell \left(\sqrt{\bar{Y}_I}, m_D, \alpha_D \right)$$

$$d_{13} = d_{33} + (1 - d_{33}) 2a_i \sup(\rho, \rho') \sin^2 \frac{\theta}{2}$$

$$d_{23} = d_{33} + (1 - d_{33}) 2a_i \sup(\rho, \rho') \cos^2 \frac{\theta}{2}$$
(5)

- for $\rho \geq \rho_s$

$$d_{33} = d_{23} = d_{13} = 1$$
(6)

where m_D, α_D are material constants, a_i is the coupling term, θ is the angle between two adjacent plies, ρ and ρ' are the transverse microcracking of two adjacent plies.

2.2. Split detection criterion

According to [3], split initiation is commonly due to high shear stress. The question is then how to specific a dominant shear location in a microcracking zone. It is supposed that within an area of sufficiently high transverse microcracking density, a split appears when the transverse microcracking density essentially due to shear has a contribution ratio being more than 75%. The choice of 75% purely represents a dominant shear state in the transverse microcracking zone. The proposed criterion is then defined at a material point M as:

$$M = \arg \max_{M \in \Omega_{0.2}} \left(\frac{\rho_{shear}}{\rho}, 0.75 \right)$$
(7)

where $\Omega_{0.2} = \{M \in \Omega_{0.2} | \rho \geq 0.2\}$ and ρ_{shear} is the transverse microcracking subjected to the shear stress.

3. Illustration

This section presents numerical computation of tensile tests on an open hole quasi-isotropic $[45_4/90_4/-45_4/0_4]_s$ specimen with 3.175 mm diameter performed by Hallett et al. [4] and a double-edge-notched $[90/0]_s$ one with 10 mm notch length carried out by Kortschot et al. [5]. The former with a thicker ply thickness facilitates intraply matrix crack formation and delamination whereas the later with a thinner ply thickness typically suppresses the damage process. For these reasons, the failure of the notched specimen is dominated by fibre breakage while the matrix dominated failure occurs in the open hole one.

The Fig. 1 illustrates the numerical investigation using ρ and ρ_{shear} maps for split detection on the open hole specimen. It is clearly shown that the ρ_{shear} to ρ ratio is 100% in the 45° and 0° plies along with the fiber direction. The split process should be then correctly modeled in the 45° and 0° plies by introducing interface elements. On the other hand, the homogenized representation is suitable for representing the transverse cracks in the 90° and -45° plies. Similarly, split investigation was performed on the $[90/0]_s$ notched specimen and the interface elements are introduced in the 0° ply to model split propagation. The computation is then relaunched at the beginning of load with the introduced cohesive element at the locations detected by split investigation.

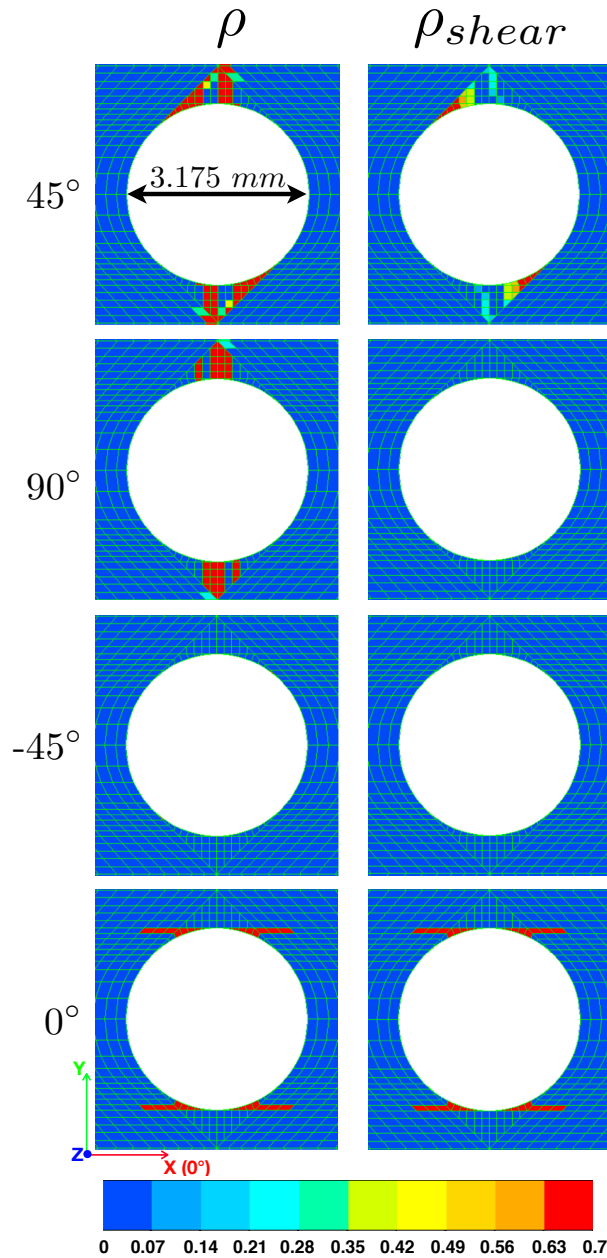


Figure 1. Illustration of the numerical investigation for split locations in $[45_4/90_4/-45_4/0_4]_s$ open hole specimen with 3.175 mm diameter

The Fig. 2 shows computational results obtained by the new split approach for the open hole laminate in comparison with the experimental observation. The appearance of the predicted stress-strain curve showing two significant load drops before fiber breakage is quite similar to the experiment one. At the first load drop, it is observed that the extensive -45/0 delamination propagates instantaneously to the free edges in an asymmetric manner as clearly seen from the X-ray image of damage. After the second load drop, the delamination occurs throughout the entire gauge section. The predicted phenomena are well coherent with the experiment. Moreover, the failure stress defined as the first load drop greater than 5% by the authors (i.e. the first drop due to asymmetrically extensive -45/0 delamination in this case) is correctly predicted by the new split approach (see Fig. 2). It should be noted that according to the authors, the load drop greater than 5% is sufficiently serious because of the loss of structure integrity despite the fact that the structure is totally failed at the higher load by the fiber breakage in the 0° ply [4]. Therefore, the global behavior after the two large drops is not quite interested in the simulations.

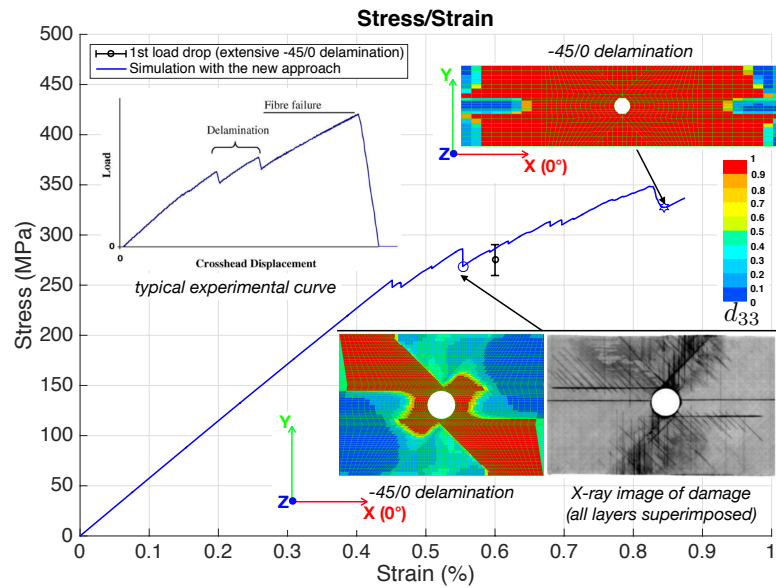


Figure 2. Stress/strain curve obtained by the new split approach compared to the experimental observation for the quasi-isotropic open hole specimen (matrix dominated failure).

The Fig. 3 shows the stress/strains curves obtained by the classical and the new approaches in comparison with the experimental strength. It is shown that the classical approach results in the too conservative strength for this specimen while the predicted strength obtained by the new split approach is well coherent with the experiment. The damage amount for this configuration is limited so that the final failure is dominated by fiber breakage in the 0° ply.

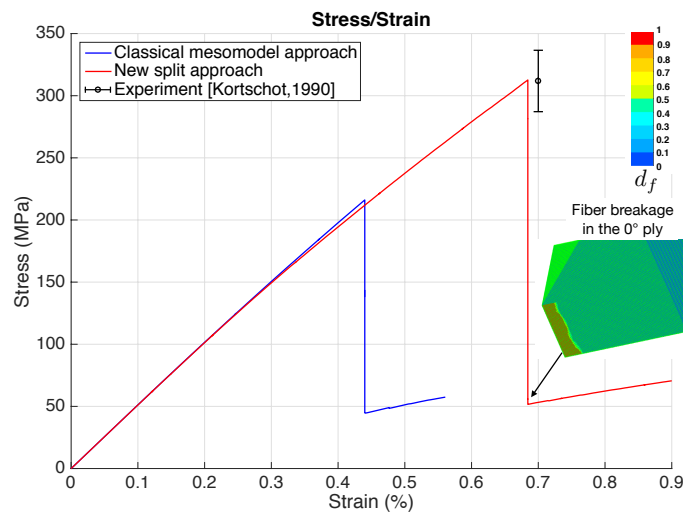


Figure 3. Stress/strain curves obtained by the classical and the new split approaches compared to the experimental strength for the [90/0]_s notched specimen (fiber dominated failure).

4. Conclusion

It has been proved that the new split approach is able to correctly model composite structures involving extensive splitting by means of two examples on the distinction of the failure modes. The locations of splits can be predicted by the classical mesomodel with the shear-based split detection criterion. The split propagation should be modeled by a discontinuous approach such as the interface elements in this research. The disadvantage is that mesh must be aligned with splits for which the XFEM-based could be more efficient.

References

- [1] P. Ladevèze, D. Néron, H. Bainier. *A virtual testing approach for laminated composites based on micromechanics*. Springer, 2017.
- [2] J.A. Nairn. *Matrix Microcracking in composites*. Elsevier Science, 2000.
- [3] J. G. Goree, M. W. Jeffrey. Longitudinal splitting in unidirectional composites, Analysis and Experiments. *NASA Contractor Report 3881 Grant NSG-1297*, 1–114, 1985.
- [4] S. Hallett, B. Green, W. Jiang, M. R. Wisnom. An experimental and numerical investigation into the damage mechanisms in notched composites. *Composites: Part A*, 40 613–624, 2009.
- [5] M. T. Kortschot, P. W. R. Beaumont. Damage mechanics of composite materials: I-measurements of damage and strength. *Composites Science and Technology*, 39 289–301, 1990.